RAPID COMMUNICATIONS

PHYSICAL REVIEW B VOLUME 49, NUMBER 19 15 MAY 1994-I

One-dimensional electron channels in the quantum limit

H. Drexler, W. Hansen, S. Manus, and J. P. Kotthaus
Sektion Physik, Ludwig-Maximilians-Universität, Geschwister-Scholl-Platz 1, D 80539 München, Germany

M. Holland and S. P. Beaumont
Department of Electronics and Electrical Engineering, University of Glasgow, Glasgow G128QQ, United Kingdom
(Received 13 September 1993; revised manuscript received 8 November 1993)

We report the results of capacitance measurements on quantum wires in which only the lowest one-dimensional subband is occupied. The wires are generated in metal-insulator-semiconductor-field-effect-transistor-type AlAs/GaAs heterojunctions with an interdigitated gate. In such devices strong lateral confinement and a well-defined threshold voltage are achieved. In the quantum limit at very low electron density the capacitance signal recorded as a function of the gate voltage exhibits a substructure that we discuss in view of a drastic change of the effective channel width when the wire starts to be occupied. At very high magnetic fields we observe spin polarization of the lowest subband. The position of the capacitance minimum that corresponds to the minimum of the density of states between the spin-polarized subbands clearly reflects the asymmetry of the one-dimensional density of states that even persists at high magnetic fields.

The density of states (DOS) of electron inversion systems in semiconductor heterostructures is relatively low compared to metallic electrodes. As a consequence, the thermodynamic DOS contributes significantly to the capacitance of the electron system measured with respect to external electrodes. This has, e.g., been demonstrated in measurements of the capacitance of two-dimensional (2D) electron systems in high magnetic fields where the thermodynamic DOS is strongly modified by the formation of Landau levels.[1] Capacitance studies on 2D electron systems have revealed very intriguing results such as gaps[2] in the DOS or a negative[3] DOS at distinct low electron densities. The capacitance of electron systems with even lower dimensionality—so-called quantum wires[4] and quantum dots[5,6]—has also been studied experimentally. If the lateral extent of 2D electron systems is reduced in one dimension so that quantum wires are formed the formerly constant DOS gradually transforms into the 1D subband structure with maxima in the DOS at the subband onsets. This results in oscillations of the capacitance as has been observed in the gate voltage derivative of the capacitance signal measured as a function of the gate voltage.[4] In those experiments the derivative was recorded because the oscillations were hardly discernible in the direct capacitance signal. Furthermore, in the gate voltage region in which the electron wire is in the 1D quantum limit, i.e., only a single 1D subband is occupied, the derivative signal is obscured by the strong capacitance onset. Here we report the results of capacitance investigations on quantum wires generated in structures especially designed so that the oscillations are very clearly resolvable even in the direct capacitance signal. We observe spin splitting and an additional feature in the capacitance signal when the electron system is in the quantum limit.

The samples used in this study are MISFET (metal-insulator-semiconductor-field-effect-transistor) -type GaAs/AlAs heterostructures similar to those employed in previous far-infrared studies.[7,8] The essential layer sequence of the MISFET is depicted in Fig. 1(b). The GaAs buffer contains a back contact formed by a 20-nm-thick layer of highly (4×10^{18} cm^{-3}) doped GaAs, with respect to which the gate voltages are applied. The low-dimensional electron system is generated at the interface between the GaAs spacer and the blocking barrier which consists of a 32-nm-thick AlAs/GaAs short-period super-

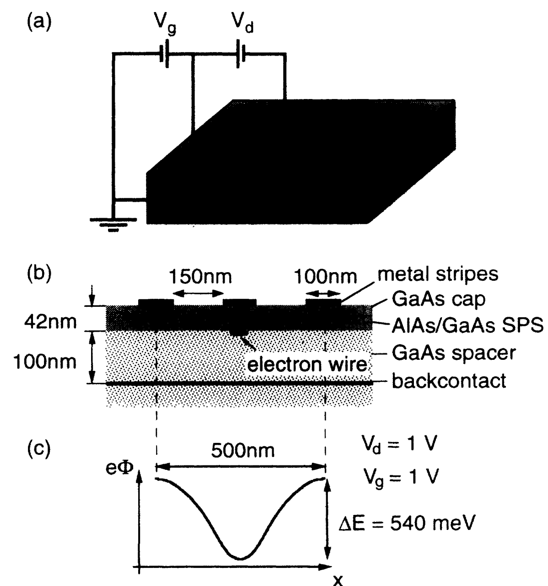

FIG. 1. (a) Sketch of the interdigitated gate geometry on top of the sample and the voltage sources applied at the electrodes. (b) Cross section of the sample. The electron wires are generated beneath the center gate biased at voltage V_g. The side gates are biased with respect to this gate by a voltage V_d. (c) The calculated bare potential induced by the gate configuration in (b) at the location of the electron wires with gate voltages as indicated.

 ©1994 The American Physical Society

lattice [7 × 9 monolayers (ML) AlAs, 6 × 9 ML GaAs]. The spacer is 100 nm thick and forms a shallow tunnel barrier through which the electron system is charged from the back contact. The structure is completed by a 10-nm-thick GaAs cap layer.

For the generation of 1D electron systems we fabricated interdigitated gate electrodes by high-resolution electron beam lithography. The geometry of the interdigitated gate is illustrated in Fig. 1(a). It is formed by two interlocked fingergates and each of them consists of 300 metal stripes of 100 nm width, 500 nm period, and with 180 μm length, respectively. One-dimensional electron wires are generated beneath a fingergate if it is biased with respect to the back contact by a voltage V_g that is larger than a distinct turn-on voltage of typically 1 V. The potential of the second fingergate tunes the lateral confinement of the electron wires. In our experiments the second fingergate is biased by a voltage V_d with respect to the first one. The potential modulation induced by the fingergates at the location of the quantum wires is indicated in Fig. 1(c). The trace is calculated with a Poisson solver neglecting the contribution of the electrons in the wires to the potential. The amplitude of the potential superlattice is about 270 meV for typical values of the voltages $V_g = V_d = 1$ V.

We measure the capacitance between the fingergate beneath which the electron wires are induced and the back contact with a small excitation voltage $dV = 5$ mV modulated at a frequency of 250 Hz$\leq f \leq$ 50 kHz and added to the gate voltage V_g. In the above frequency range the alternating current through the sample is always 90° out of phase to the excitation voltage ensuring that the signal is proportional to the differential capacitance $C = dQ/dV_g$ and the resistance of the tunnel barrier does not affect the signal. The voltage difference V_d between the two fingergates is kept fixed at $V_d = 1$ V for the data presented here. Consequently, the carrier density of the 1D electron systems is varied with the gate voltage V_g whereas the potential landscape induced by external charges is held almost constant.

In Fig. 2 we depict the capacitance of our device at different magnetic fields as a function of the gate voltage V_g. The data are taken at a temperature of 4.2 K and the gate voltage V_g is modulated at a frequency $f = 10$ kHz. Below the turn-on voltage $V_g \approx 1.13$ V the measured capacitance is determined by the geometry of the gate electrode and the back contact alone. If the gate voltage is increased above the turn-on voltage the capacitance rises abruptly because the electron systems generated at the junction between spacer and blocking barrier now contribute to the capacitance.

In model calculations in which the electrodes have been replaced by thin metallic sheets we find that the contribution of the wire capacitance to the measured capacitance is very large as soon as the wires are formed. As mentioned above, this contribution depends not only on the wire geometry but also on the DOS in the quantum wire. The capacitance per wire length can be viewed as a geometric capacitance C_{geo} in series with a capacitance $C_{\text{DOS}} = e^2 D$ proportional to the density of states D in the electron system at the chemical potential:

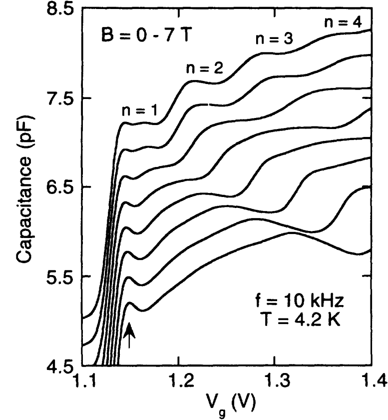

FIG. 2. Capacitance of the wire array recorded as function of the gate voltage V_g at different magnetic fields that are increased in steps of 1 T from the top to the bottom trace. The scale refers to the top trace ($B = 0$ T) and a constant offset is subtracted from the traces at finite fields for clarity. The values n indicate the subband that start to be filled in the corresponding gate voltage regimes. The maximum highlighted by the arrow is discussed in the text.

$C_w^{-1} = C_{\text{geo}}^{-1} + C_{\text{DOS}}^{-1}$. Oscillations of the thermodynamic DOS in the quantum wires thus cause oscillations of the capacitance signal. The ideal DOS of the nth subband $D_n(E)$ is proportional to $1/\sqrt{E - E_n}$ with the subband edges E_n. At an energy of, e.g., 5 meV above E_1, the ideal DOS in the first subband corresponds to a capacitance $C_{\text{DOS}} = e^2 D_1(5 \text{ meV}) \approx 1$ nF/m. This value is about 7 times larger than the geometrical capacitance which we derive from the experimental data as discussed later. The observed smooth form of the steps can be explained with a broadened DOS. We point out furthermore that the geometrical capacitance changes with the channel occupation as well so that the steplike form of the capacitance signal observed in Fig. 2 does not simply reflect the DOS as function of the channel occupation. We consider the widening of the electron wires in the lateral direction as the most important origin of the increase of the geometrical capacitance with increasing wire occupation. The decreasing distance between the gate and the center of charge of the electron gas causes an additional smooth and monotonical growth of the capacitance with increasing gate voltage.

The data of Fig. 2 may thus be understood as follows: With increasing gate voltage the DOS in the 1D subband that is presently filled decreases and causes a reduction of the measured capacitance C_w below C_{geo}. If a new subband starts to be occupied the large DOS at the onset of the subband causes the capacitance to approach the value of the geometrical capacitance, which itself rises due to the alteration of the wire geometry. Thus the steps in the capacitance signal clearly identify the voltages where the first, second, third, and fourth subband start to be filled. The indices n in Fig. 2 denote the highest occupied subband in the voltage ranges of the $B = 0$ T trace. We note that, unlike in previous studies on quantum wires, here pronounced oscillations are observed in the direct capacitance signal even at $T = 4.2$ K rather than in its

voltage derivative at $T = 0.5$ K.[4] This demonstrates that in our electron wires the effect of the lateral quantization clearly dominates the effect of disorder.

In a magnetic field oriented perpendicular to the sample surface the 1D subbands transform into hybrid bands with a DOS and level separation that are increasingly ruled by the magnetic field. For a rough estimate of the subband spacing from the data of Fig. 2 we assume that the effective confinement potential is parabolic with constant subband spacing $\hbar\omega_0$ at densities, where the wires are in the 1D quantum limit. Then in a magnetic field the level separation increases as $\hbar\omega = \hbar\sqrt{\omega_0^2 + \omega_c^2}$ with the cyclotron frequency $\omega_c = eB/m^*$. The number of electrons which can be filled into the lowest subband without occupying the second subband is found to be

$$n_{ql} = \sqrt{8m^*/\pi^2\hbar}\frac{(\omega_0^2 + \omega_c^2)^{3/4}}{\omega_0}. \quad (1)$$

Accordingly, with increasing magnetic field n_{ql} increases and thus also the gate voltage at which the second subband starts to become occupied. The capacitance C_w of our sample is observed to be nearly constant in the gate voltage range where only the first subband is occupied. Hence the n_{ql} may also be approximated by

$$n_{ql} = C_w U_{ql}/e, \quad (2)$$

where U_{ql} is the difference between the threshold voltage and the voltage at which the second subband starts to be filled. With Eqs. (1) and (2) the voltage U_{ql} at which the second subband starts to become occupied can be expressed as function of the cyclotron frequency ω_c. The values for the subband spacing $\hbar\omega_0$ at $B = 0$ T and the capacitance C_w that best describe the onsets of the second subband in Fig. 2 are $\hbar\omega_0 = 4.7$ meV and $C_w = 140$ pF/m, respectively.

The high homogeneity of our sample allows us to resolve an additional structure highlighted by an arrow in Fig. 2. It occurs at gate voltages that correspond to very low electron densities in the electric quantum limit. The arrow points to a maximum position although at first sight it might be tempting to perceive the feature as a capacitance minimum at higher gate voltages. However, we argue in the following that the feature results from an enhancement of the capacitance signal at gate voltages where the channel has just been formed and rapidly changes geometry. In 2D electron systems generated with homogeneous gates on the same wafer material we do not observe such a peak. Thus we interpret this structure as a characteristic of 1D electron systems. Since the peak is already observed at $T = 4.2$ K we consider it unlikely that it reflects a special electron configuration such as a charge density wave or a Wigner crystal. Instead we attribute it to the renormalization of the effective electron potential via the electron-electron interaction. With increasing electron density the repulsive electron interaction flattens the effective potential in the middle of the channel.[9] The channel becomes wider and, accordingly, a larger capacitance is measured at higher gate voltages. A rapid change of the geometrical capacitance in a small gate voltage range can cause a considerably enhanced capacitance dQ/dV_g per wire length according to

$$dQ/dV_g = C_w[1 + (Q_w/C_{\text{geo}}^2)(dC_{\text{geo}}/dV_g)],$$

where Q_w is the 1D charge density on the quantum wire.

The renormalization of the effective confinement potential influences not only C_{geo} but also C_{DOS}. With a widening of the effective confinement potential the subband energy and thus also the chemical potential as measured from the GaAs conduction-band edge, i.e., from the bottom of the confining potential, are reduced. This reduction counteracts the growth of the chemical potential with increasing electron density in the wire, which is reflected by the finite C_{DOS} in our model. The renormalization of the subband energy thus results in an increased capacitance signal.

The behavior of the capacitance peak with magnetic field is in correspondence with our interpretation. The localization of the electron wave function on the scale of the magnetic length $l_h = \sqrt{\hbar/eB}$ results in screening properties that become more similar to a classical plasma. We, therefore, expect the effective channel width to be reduced below the zero-field value at low density and an even more rapid change of the channel width with increasing electron density. On the other hand, the subband structure is dominantly determined by the magnetic energy $\hbar\omega_c$ at high magnetic fields and, therefore, the change of the chemical potential caused by renormalization of the effective confinement is reduced. Thus the influence of the subband structure on C_{DOS} is reduced with increasing magnetic field. Correspondingly the impact of the channel widening on the capacitance should become more pronounced at high magnetic field while the voltage range at which it appears should not change strongly. Both are observed in the data of Fig. 2.

In Fig. 3 we present data recorded at high magnetic

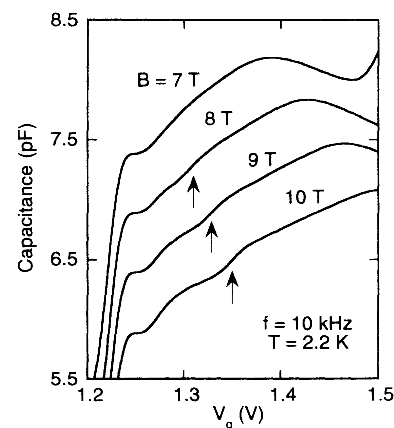

FIG. 3. Sample capacitance recorded at high magnetic fields and a temperature of $T = 2.2$ K. The arrows highlight the steps in the capacitance that arise from occupation of the second spin-polarized 1D subband. The scale refers to the trace recorded at $B = 7$ T and a constant offset is subtracted from the traces at $B \geq 8$ T for clarity. The sample is the same as in Fig. 2. The fact that in these measurements the peak at low densities is weaker is attributed to increased potential fluctuations within the sample after thermal cycling.

fields ($B \geq 7$ T) where an additional step in the capacitance traces gradually becomes observable. Although weaker than the other features in our capacitance data this step is clearly resolved at $B \geq 9$ T. We attribute this feature to the spin splitting of the lowest 1D subband. The energy splitting between the spin-polarized subbands is usually described as $\Delta E = g\mu_B B$ with the Bohr magneton μ_B and the electronic Landé g factor. In capacitance data measured at 2D electron systems as a function of the gate voltage, a minimum occurs at precisely half the electron density of the totally occupied spin-degenerate Landau level. This is well understood assuming symmetric broadening of the Landau levels. At odd filling factors each spin-split state of the same Landau level is partly occupied and the sum of both is equal to half the electron density in a completely filled Landau level. The capacitance minimum measured in 2D systems at odd filling factors is much weaker than at even filling factor because the Landau-level separation is much larger than the spin splitting. Thus if the Landau levels are broadened, the DOS is considerably higher at odd filling factors.[1] Since the DOS between 1D hybrid subbands is always finite it is not surprising that the feature observed in our wire system is weak.

The experimental data of Fig. 3 demonstrate that the 1D character of our electron wires persists to high magnetic fields. The step in the capacitance signal occurs at far lower gate voltage than half the gate voltage above turn-on voltage at which the second subband starts to be occupied. With the capacitance C_w we calculate at $B = 10$ T a one-dimensional electron density of about 1.1×10^6 cm^{-1} at the position of the step whereas the filling of the second subband is expected at $n_{ql} = 4.1 \times 10^6$ cm^{-1}. Whereas it is generally assumed that 2D Landau levels are symmetrically broadened around their center energy, a 1D subband, even if broadened and subjected to a magnetic field, will have an asymmetric DOS. Thus at the gate voltage where the step is observed, the number of electrons already filled into the second spin-polarized 1D subband is much less than the number of empty states in the lower spin-polarized 1D subband. Accordingly, the 1D electron density at the step is much smaller than $0.5n_{ql}$.

Without broadening of the 1D DOS the first spin-polarized subband needs to be filled until the chemical potential is lifted by $\Delta E = g\mu_B B$ beyond the subband edge in order to start occupation of the second spin-polarized subband. The corresponding electron density strongly depends on the quantization energy $\hbar\omega_0$ at $B = 0$ T and the effective g factor. This is in contrast to the 2D case where the electron density at filling factor 1, where the Fermi level lies in the minimum of the DOS between the lowest two spin-split Landau levels, is only a linear function of the magnetic field. With the assumption of an ideal unbroadened 1D DOS and an effective parabolic potential, a carrier density of 1.1×10^6 cm^{-1} yields a Fermi level which lies 4.8 meV above the subband energy. This energy being equal to the spin splitting yields a g factor of $g = 8.4$. This result may be modified if a different confinement potential is assumed or if the broadening of the DOS is taken into account. We note that the value found with our assumption is comparable to those reported for 2D electron systems[10,11] but different from a value found with a different method for even wider wires in a recent publication.[12]

We are very grateful to A. Schmeller for help in the lithography and to V. Dolgopolov for helpful discussion. Financial support of the Deutsche Forschungsgemeinschaft is gratefully acknowledged.

[1] T. P. Smith, B. B. Goldberg, P. J. Stiles, and M. Heiblum, Phys. Rev. B **32**, 2696 (1985).

[2] R. C. Ashoori, J. A. Lebens, N. P. Bigelow, and R. H. Silsbee, Phys. Rev. Lett. **64**, 681 (1990).

[3] S. V. Kravchenko, P. M. Pudalov, and S. G. Semenchinsky, Phys. Lett. A **141**, 71 (1989); S. V. Kravchenko, D. A. Rinberg, and S. G. Semenchinsky, Phys. Rev. B **42**, 3741 (1990).

[4] T. P. Smith III, H. Arnot, J. M. Hong, C. M. Knoedler, S. E. Laux, and H. Schmid, Phys. Rev. Lett. **59**, 2802 (1987).

[5] W. Hansen, T. P. Smith III, K. Y. Lee, J. A. Brum, C. M. Knoedler, J. M. Hong, and D. P. Kern, Phys. Rev. Lett. **62**, 2168 (1989).

[6] R. C. Ashoori, H. L. Störmer, J. S. Weiner, L. N. Pfeiffer, K. W. Baldwin, and K. W. West, Phys. Rev. Lett. **71**, 613 (1993).

[7] H. Drexler, W. Hansen, J. P. Kotthaus, M. Holland, and S. P. Beaumont, Semicond. Sci. Technol. **7**, 1008 (1992).

[8] H. Drexler, W. Hansen, J. P. Kotthaus, M. Holland, and S. P. Beaumont, Phys. Rev. B **46**, 12 849 (1992).

[9] S. E. Laux and F. Stern, Appl. Phys. Lett. **49**, 91 (1986).

[10] R. J. Nicholas, R. J. Haug, K. v. Klitzing, and G. Weimann, Phys. Rev. B **37**, 1294 (1988).

[11] A. Pinczuk, B. S. Dennis, D. Heiman, C. Kallin, L. Brey, C. Tejedor, S. Schmitt-Rink, L. N. Pfeiffer, and K. W. West, Phys. Rev. Lett. **68**, 3623 (1993).

[12] J. Wrobel, F. Kuchar, K. Ismail, K. Y. Lee, H. Nickel, W. Schlapp, G. Grabecki, and T. Dietl, Surf. Sci. (to be published).

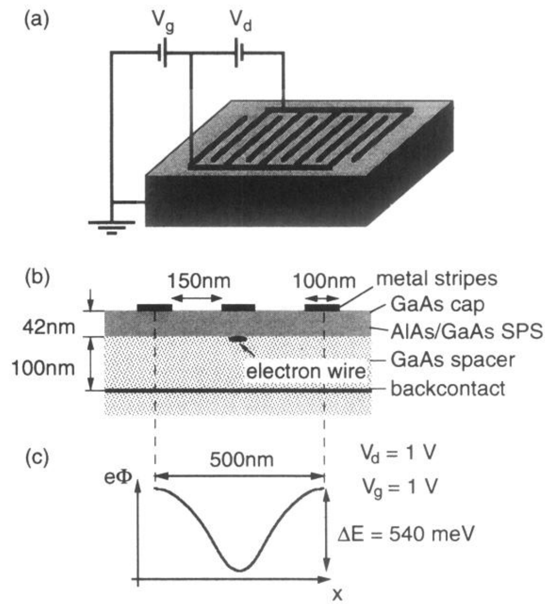

FIG. 1. (a) Sketch of the interdigitated gate geometry on top of the sample and the voltage sources applied at the electrodes. (b) Cross section of the sample. The electron wires are generated beneath the center gate biased at voltage V_g. The side gates are biased with respect to this gate by a voltage V_d. (c) The calculated bare potential induced by the gate configuration in (b) at the location of the electron wires with gate voltages as indicated.